Article
Vol. 25, No. 6, p. 849–862, December 2021
https://doi.org/10.1007/s12303-021-0012-8
pISSN 1226-4806 eISSN 1598-7477
Geosciences Journal GJ

Zircon U-Pb geochronology, geochemistry, and Hf isotopic compositions of the trachyandesite in the Dong'an Au deposit, Lesser Xing'an Range, northeastern China

Gantian Li[1], Fengyue Sun[1], Bile Li[1,2]*, Yonggang Sun[1], and Runtao Yu[1]

[1]College of Earth Sciences, Jilin University, Changchun 130061, China
[2]Key Laboratory of Mineral Resources Evaluation in Northeast Asia, Ministry of Land and Resources, Changchun 130061, China

ABSTRACT: The Dong'an Au deposit is a large-sized epithermal Au deposit discovered in the Lesser Xing'an Range, Northeastern China. Intermediate–acid volcanic rocks (e.g., trachyandesite, andesite, dacite, rhyolite, and rhyolitic tuff) of the Lower Cretaceous Fuminghe Formation are the important surrounding rocks for Au mineralization in the Dong'an Au deposit. However, the relationship between the intermediate volcanic rocks and the acidic volcanic rocks is unclear. The authors present new geochemical, zircon U-Pb and Hf isotope data for the trachyandesites in the Dong'an Au deposit. The whole-rock geochemical data indicate that the trachyandesite samples are high-K calc-alkaline. They are enriched in LILEs (e.g., K, Rb, and Ba), LREEs, and incompatible elements (e.g., Th and U), but are depleted in HFSEs (e.g., Nb, Ta, P, and Ti), showing characteristics of volcanic arc magmas. They have low $Mg^{\#}$ values (32.77–48.12), Cr, Ni, and Co contents. Zircons U-Pb dating of the trachyandesites from sample DA-N_1 and DA-N_2 yield weighted average ages of 108.0 ± 1.1 Ma (MSWD = 0.91) and 104.7 ± 4.3 Ma (MSWD = 17). In situ zircon Hf isotope analyses of the trachyandesites from sample DA-N_1 and DA-N_2 yield $\varepsilon_{Hf}(t)$ values of –3.2 – 1.2 and –2.3 – 2.6, and two-stage model age (T_{DM2}) of 1372–1090 Ma and 1321–1009 Ma, respectively. These suggest the trachyandesite were derived from partial melting of the juvenile lower crust with involvement of the ancient crustal materials. Combined with previous geological and petrogeochemical characteristics of the Lower Cretaceous Fuminghe Formation volcanic rocks in the Dong'an Au deposit, the Fuminghe Formation volcanic rocks are believed to be comagmatic, and fractional crystallization played an important role in the differentiation of these volcanic rocks. They were likely formed during the retreat of the subducted Paleo-Pacific Plate.

Key words: Lesser Xing'an Range, Dong'an Au deposit, trachyandesite, geochemistry, zircon U-Pb age, Hf isotope

Manuscript received July 26, 2020; Manuscript accepted April 28, 2021

1. INTRODUCTION

Dong'an epithermal Au deposit was newly discovered by No. 707 geology exploration team for nonferrous metal, Heilongjiang Province. The 5# vein within the deposit hosts about 24 t gold reserves. Discovery of Dong'an Au deposit led to a significant increase in mineral exploration and research into epithermal mineralization in the Lesser Xing'an Range, and then a number of epithermal Au deposits were found in recent years. Previous studies proposed that the majority of the epithermal mineralization concentrated during the late Early Cretaceous in the Lesser Xing'an Range (Chen, 2011; Xu et al., 2013), all the epithermal mineralization in the volcanic rocks occurs during the waning stage of the volcanic events (Sun et al., 2013a; Liu et al., 2021), and both of the mineralization and volcanism formed in a uniform tectonic setting (Li et al., 2012).

Intermediate–acid volcanic rocks (e.g., trachyandesite, andesite, dacite, rhyolite, and rhyolitic tuff) of the Lower Cretaceous Fuminghe Formation are the important surrounding rocks that host the majority of mineralization in the Dong'an Au deposit. However, in the Dong'an Au mining area, little is known about the coeval magmatic processes, the relationship between the

*Corresponding author:
Bile Li
College of Earth Sciences, Jilin University, 2199 Jianshe Street, Changchun 130061, China
Tel: +86-133-5327-7179, E-mail: libl@jlu.edu.cn

Electronic supplementary material
The online version of this article (https://doi.org/10.1007/s12303-021-0012-8) contains supplementary material, which is available to authorized users.

©The Association of Korean Geoscience Societies and Springer 2021

intermediate volcanic rocks and the acidic volcanic rocks is unclear. In this paper, we present new geochemical, zircon U-Pb and Hf isotope data for the trachyandesites with the aim to clarify their magma source and tectonic setting. These new data, in combination with petrogeochemical data from coeval volcanic rocks in the Dong'an Au mining area, provide strong constraints on the magmatic processes prior to epithermal mineralization.

2. GEOLOGICAL BACKGROUND AND SAMPLING

The Dong'an Au deposit is located in the northern Lesser Xing'an Range. The Lesser Xing'an Range extends to the western boundary of the Songliao Basin and to the eastern boundary of the Mudanjiang Fault (Fig. 1; Wu et al., 2007). The main geological evolution history of the region is as follows: prior to the Palaeozoic, the crust in the area experienced several episodes of supercontinent formation and break-up. During the Early Palaeozoic, the area was in a state of relatively stable uplift, with only rare instances of magmatic activity. From the late Palaeozoic to the Early Mesozoic, collision of the North China Craton with the Siberia Craton resulted in the reactivation and mobilization of metamorphic basement rocks, which led to large-scale emplacements of deep-seated magmas (Wen et al., 2013). During the Mesozoic, the region was affected by subduction of the Pacific plate, during

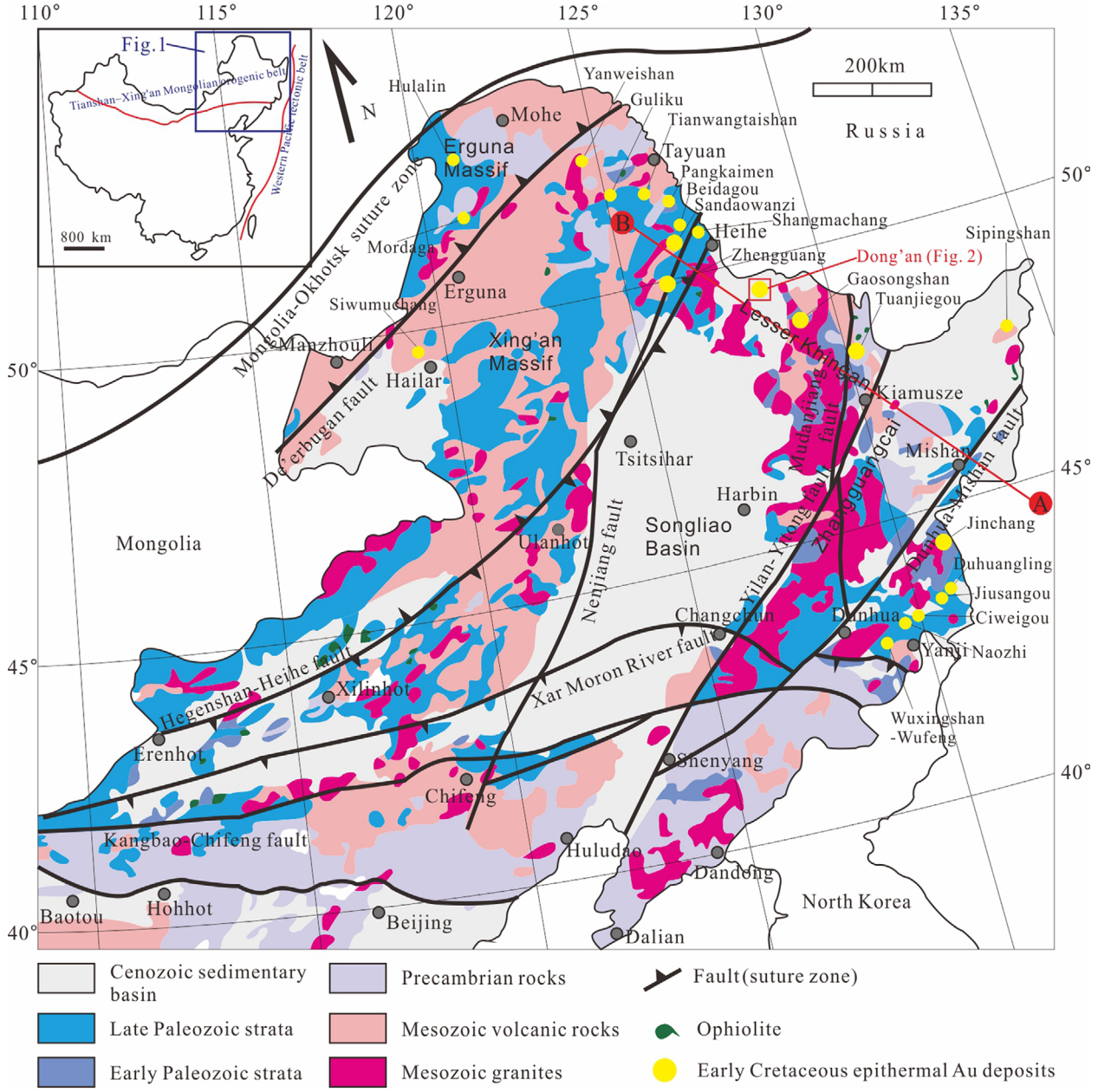

Fig. 1. Geological map showing the distribution of Early Cretaceous epithermal Au deposits in NE China (modified according to Bai et al., 2012; Chen et al., 2012; Sun et al., 2013a).

which time the area was in an extensional tectonic setting along an active continental margin, and experienced strong extensional tectonics and taphrogeny. The middle Yanshanian movement, which occurred during Late Jurassic to Early Cretaceous, was especially strong, and was accompanied by large-scale fault activities (Ye, 2011). The regional lithospheric faults were strongly mobilized during this time, resulting in the formation of a series of NE-, NW-, NNE-striking crustal faults and the Wudihe Basin, associated with extrusions of intermediate to intermediate–acid volcanic rocks and the formation of volcanic edifices (Huo and Sun, 2010). The tectonic setting was especially favourable for various types of mineralization, including the hydrothermal mineralization of precious and nonferrous metals (e.g., Mo, Cu, and Au). This period, which climaxed during Early Jurassic to Early Cretaceous, yielded a variety of porphyry molybdenum polymetallic and epithermal Au polymetallic deposits.

The major strata in the Dong'an Au mining area consist of intermediate–acid volcanic rocks (e.g., trachyandesite, andesite, dacite, rhyolite, and rhyolitic tuff) of the Lower Cretaceous Fuminghe Formation, which are broadly located in the center of the Au mining area, close to ore bodies, constituting major host rocks of the Dong'an Au deposit. The other strata include sandy conglomerate of the Tertiary Sunwu Formation, the basalts of the Quaternary Daxiongshan Formation, and the Quaternary sediments. The major exposed intrusions consist of Early Jurassic medium–coarse grained alkali-feldspar granite (176.3 ± 1.1 Ma; Zhi et al., 2016) and fine-grained alkali granite (173.8 ± 1.9 Ma; Xue et al., 2012), and Early Cretaceous rhyolite porphyry (108.1 ± 2.4 Ma; Zhang et al., 2010) (Fig. 2). Generally, gold orebodies are thought to be spatially associated with the rhyolite porphyries (Fig. 2; Zhang et al., 2010). Faults and volcanic edifices are the major geological structures in the Au mining area. Three groups of NE-, near SN-, NNW-striking faults, which are secondary faults of the NNE-striking Kuerbin deep-seated fault, are the main structural and ore-conducting features that controlled the formation and emplacement of the fine-grained alkali granite, the rhyolite porphyry, and the volcanic edifices. The fault structures, especially near SN-striking fault, is the main ore-hosted structure

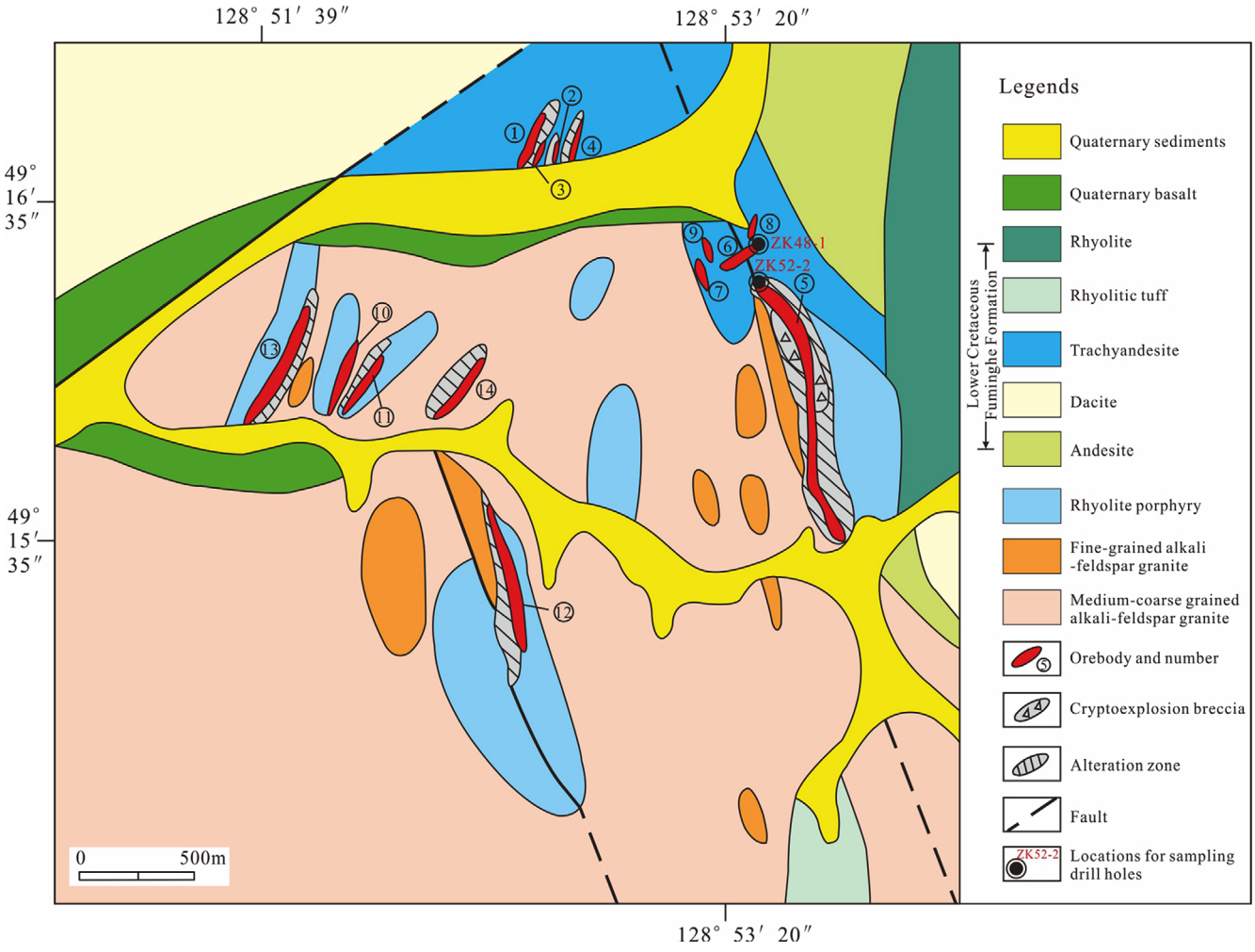

Fig. 2. Geological map of the Dong'an Au mining area (modified after Xue et al., 2002).

https://doi.org/10.1007/s12303-021-0012-8

of Dong'an Au deposit, and the hydrothermal cryptoexplosive breccias are also provided space favourable for mineralization.

14 gold-bearing veins have been discovered in this Au mining area, most of them are hosted by the volcanics, with lesser amounts of mineralization hosted by Early Jurassic alkali-feldspar granites. The largest orebody is occurred in vein 5#, and has a length of nearly 770 m, a maximum known depth of 358 m, and an average width of 6.70 m. The orebody of the vein 5# is near SN-striking, dips steeply to the east in the northern part but to the west in the south at angles of 70–89°. The mineralization in this orebody has average Au and Ag grades of 9.05 g/t and 75.8 g/t, respectively; and the contents of the Au and Ag show a positive correlation with each other (correlation coefficient of 0.786; Guo et al., 2004). The alteration types of host rock are silicification, adularia, sericite, and chlorite, and dominated by silicification and adularia. The ore minerals within the deposit contain small amounts of metal sulfides (generally < 3 wt%), predominantly pyrite with lesser amounts of chalcopyrite, galena, sphalerite, argentite and acanthite, and the majority of the noble metals are present as electrum with small amounts of kustelite and native silver. The comb-like, cluster-like quartz and lumpy-like, fine and mesh vein-like adularia are major in the gangue minerals, while sericite and chlorite are minor (Xue et al., 2002; Su et al., 2006).

The samples were obtained from drill holes ZK48-1 and ZK52-2 at a depth of 480–500 m and the drilling coordinates are 128°53′33″E, 49°16′23″N and 128°53′32″E, 49°16′17″N, respectively. The trachyandesite is widely distributed within the Dong'an Au mining area. The trachyandesite samples are grey green to light gray in color, with porphyritic texture and massive structure (Fig. 3). Most samples contain 35–65% phenocrysts of mainly plagioclase and orthoclase with minor dark-rimmed biotite and hornblende, all of which vary in length between 0.1 and 1.8 mm. The feldsper phenocrysts are euhedral to subhedral in shape, and plagioclase are characterized by polysynthetic twins and carlsbad twins respectively in plagioclase and orthoclase. The matrix consists mainly of plagioclase and orthoclase crystallites and vitreous, forming hyalopilitic texture.

3. ANALYTICAL METHODS

3.1. Major and Trace Element Determinations

The major and trace element of samples were measured in the Key Laboratory of Mineral Resources Evaluation in Northeast Asia, Ministry of Land and Resources, Changchun, China. The samples were crushed to about 200 meshes after weathered surfaces removed. The major and trace element composition were tested

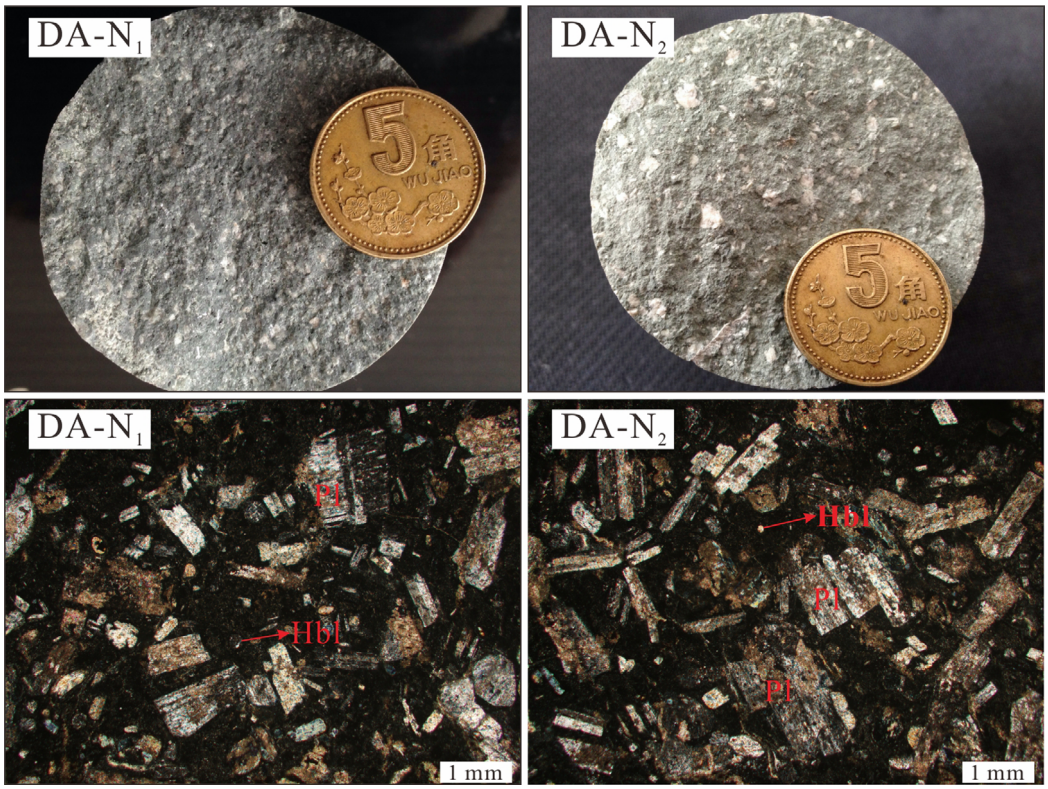

Fig. 3. Photographs and microphotographs (under cross-polarized light) of the trachyandesite samples. The size of the coin in Figure 3 is 20.5 mm. Abbreviations: Hbl = Hornblende, Pl = Plagioclase.

by X-ray fluorescence (XRF) and Agilent 7500A respectively, and analytical uncertainties range from 2–5%. The analytical results for the BHVO-1 (basalt), and BCR-2 (basalt) standards indicate that the analytical precision for major elements is better than 5%, and for trace elements, generally better than 10% (Rudnick et al., 2004).

3.2. LA-ICP-MS Zircon U-Pb Dating

The samples for zircon U-Pb data test were volcanic rock picked from drill holes in Dong'an Au mining area. Zircons were extracted from whole-rock samples using standard techniques of density separation at the Langfang Regional Geological Survey, Hebei Province, China. The zircon samples are of smooth surface with different aspect ratio and color, and handpicked under a binocular microscope.

To select the best points of isotopic analysis, zircons' characteristics of crystal morphology and internal structures are obtained through reflector and CL (cathode-luminescence) images before analysis in situ. Zircon pigeon, reflector and CL experiments were preceded in the nuclear industry & geological research institute test center, Beijing. Zircon U-Pb data was proceeded at the State Key Laboratory of Geological Processes and Mineral Resources, China University of Geosciences, Wuhan, China. Zircon U-Pb data was performed with a 32 μm laser, using He as carrier gas. The zircon 91500 and NIST SRM 610 silicate glass were using as external standard for age calibration and element content, respectively. The depth of laser ablation in zircon samples ranges from 20 to 40 μm. For detailed instruments settings and analytical procedures, see Yuan et al. (2004). The ICP-MS Data Cal (Liu et al., 2008, 2010) and Isoplot (Ludwig, 2003) programs were used for data reduction. Correction for common Pb was made following Anderson (2002). Errors on individual analyses by LA-ICP-MS are quoted at the 1σ level, while errors on pooled ages are quoted at the 95% (2σ) confidence level.

3.3. Hf Isotope Analyses

In situ zircon Hf isotope analyses were performed using a Neptune MC-ICP-MS with an ArF excimer laser ablation system (193 nm) at the State Key Laboratory of Geological Processes and Mineral Resources, China University of Geosciences, Wuhan, China. We used a simple Y junction downstream from the sample cell to add small amounts of nitrogen (4 ml mime) to the argon makeup gas flow (Hu et al., 2008a, 2008b). Compared with the standard arrangement, the addition of nitrogen in combination with the use of a newly designed X skimmer cone and Jet sample cone in Neptune Plus, improved the signal intensities of Hf, Yb, and Lu by factors of 5.3, 4.0, and 2.4, respectively. All data were acquired on zircon in single spot ablation mode with a spot size of 44 μm. Each measurement consisted of 20s of acquisition of the background signal followed by 50 s of acquisition of the ablation signal. For details of the operating conditions for the laser ablation system and the MC-ICP-MS instrument, as well as the analytical method (Hu et al., 2012).

4. ANALYTICAL RESULTS

4.1. Geochemistry

4.1.1. Major elements

The whole-rock geochemical data (Table S1 in the electronic supplementary material) indicate that the samples are felsic, and contain SiO_2 concentrations of 57.72–63.54 wt% with an average

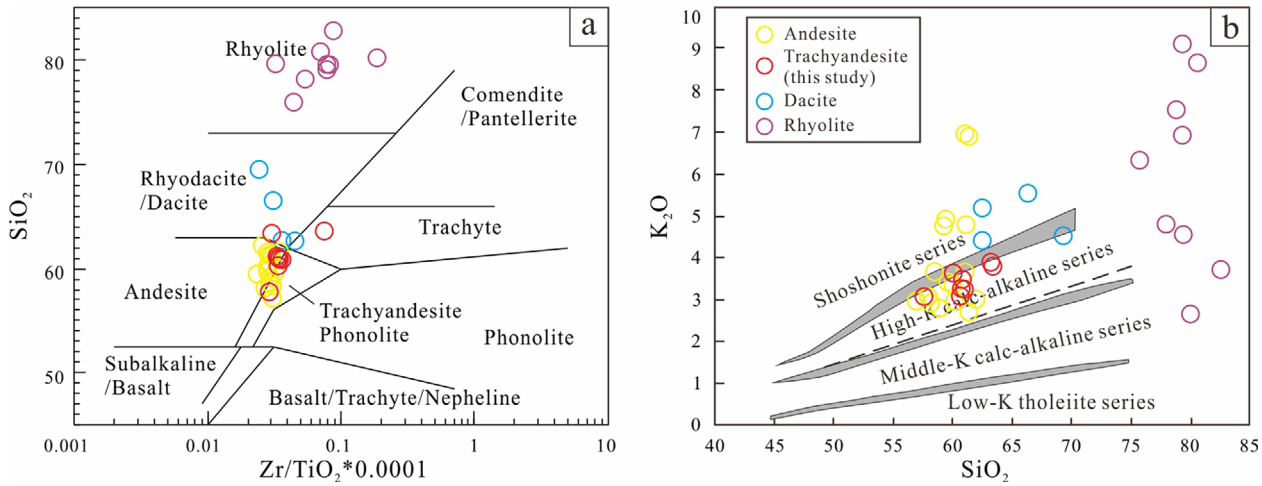

Fig. 4. (a) Plots of SiO_2 vs. (Na_2O + K_2O) (after Irvine and Baragar, 1971) and (b) SiO_2 vs. K_2O (after Peccerillo and Taylor, 1976) for the trachyandesites from the Dong'an Au mining area. The sources of the published data on the Lower Cretaceous Fuminghe Formation volcanic rocks from the Dong'an Au mining area are from Zhang et al. (2010), Liu et al. (2015), and Liu et al. (2021).

https://doi.org/10.1007/s12303-021-0012-8

of 61.07 wt%, and Al_2O_3 concentrations of 16.56–17.65 wt%. The majority of these samples are classified as trachyandesites in a $Zr/TiO_2 * 0.0001$ vs. SiO_2 diagram (Fig. 4a), although very few are classified as trachytes. They are classified as high-K calc-alkaline in a SiO_2 vs. K_2O diagram (Fig. 4b). These samples have Na_2O concentrations of 1.43–4.32 wt%, K_2O concentrations of 3.07–3.89 wt%, CaO concentrations of 2.87–4.20 wt%, and total alkali ($Na_2O + K_2O$) concentrations of 5.32–7.84 wt% with an average of 6.90 wt%.

4.1.2. Trace elements

The trace and rare earth elements (REE) compositions of the samples are given in Table S1. Chondrite-normalized REE patterns for the samples uniformly show slightly negative Eu anomalies (Eu/Eu* = 0.84–1.03) and relatively flat HREE patterns (Fig. 5a). The samples are characterized by clear fractionation of REEs, which are enriched in LREEs relative to HREEs (LREEs/HREEs = 9.37–11.26), with large REE pattern slopes $(La/Yb)_N$ = 10.77–14.24). The samples have uniform primitive-mantle normalized trace element patterns (Fig. 5b), which are significantly enriched in LILEs (e.g., K, Rb, and Ba) LREEs, and incompatible elements (e.g., Th and U), but are depleted in HFSEs (e.g., Nb, Ta, P, and Ti). They have low $Mg^{\#}$ values (32.77–48.12), and low Cr (5.33–16.00 ppm), Ni (5.94–13.11 ppm), and Co (10.79–15.70 ppm), with Rb/Sr ratios of 0.05–2.14 (mostly 0.10–0.19), Nb/Ta ratio of 1.56–21.06 (average of 9.96), Th/La ratio of 0.164–0.289 (average of 0.233), Th/Nb ratio of 0.395–0.987 (average of 0.717), and La/Nb ratio of 2.35–3.37.

4.2. Zircon U-Pb Dating

The zircons separated from sample DA-N_1 contain clear oscillatory zoning, have typical core-rim structures, and have euhedral bipyramidal and integrated crystal shapes, indicating a magmatic origin. In comparison, the zircons separated from sample DA-N_2 appear clear and the majority have long columnar shapes, although some are stumpy and granular (Fig. 6). The compositional data for these zircons are given in Table S2 (electronic supplementary material), and Th/U ratios of zircons are between 0.58–2.08 (average of 1.14; DA-N_1: 0.61–2.08, DA-

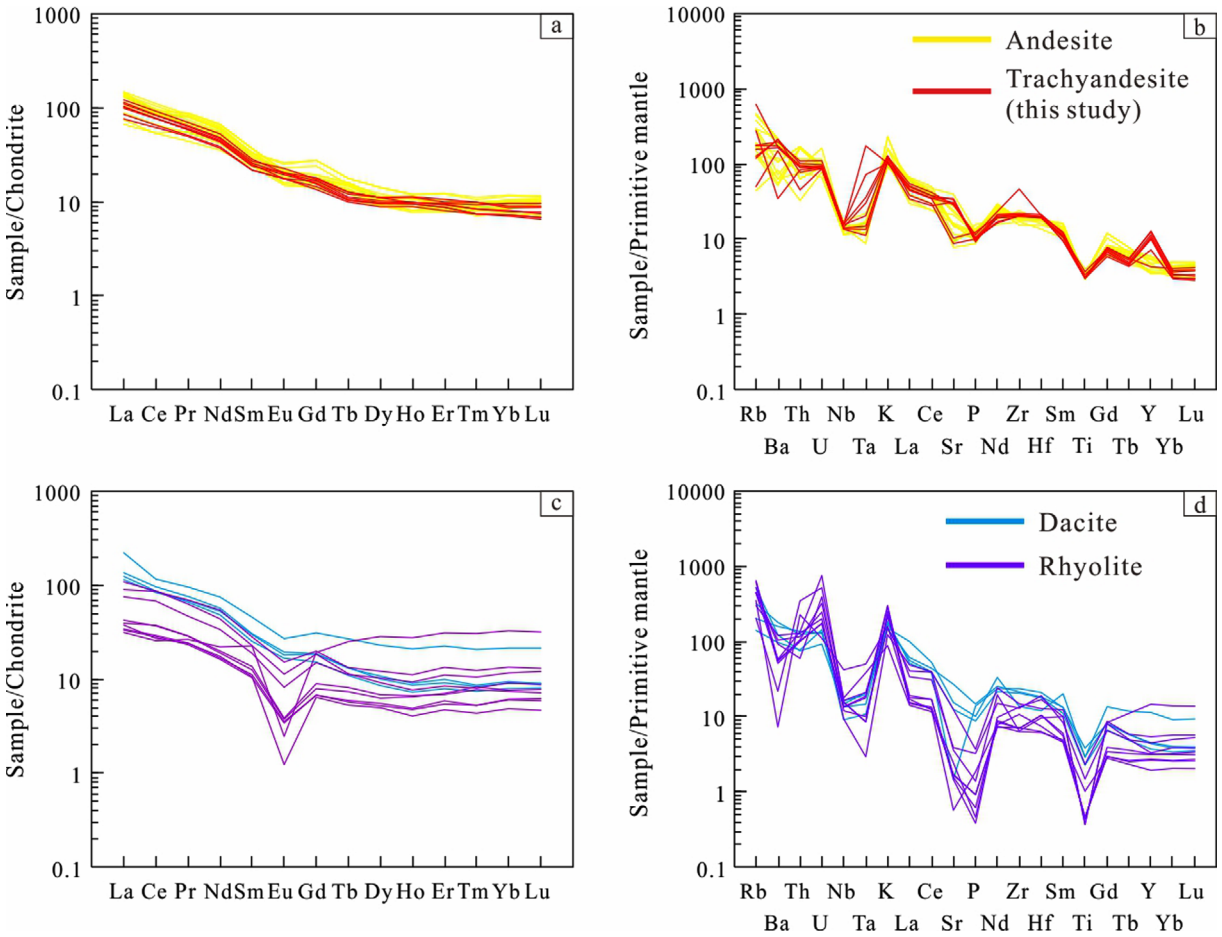

Fig. 5. Chondrite-normalized REE patterns (a) and primitive-mantle-normalized trace elements spider diagrams (b) for the trachyandesites and the Lower Cretaceous Fuminghe Formation volcanic rocks from the Dong'an Au mining area (chondrite and primitive-mantle values are from Boynton (1984) and Sun and McDonough (1989), respectively). The data sources are the same as those in Figure 4.

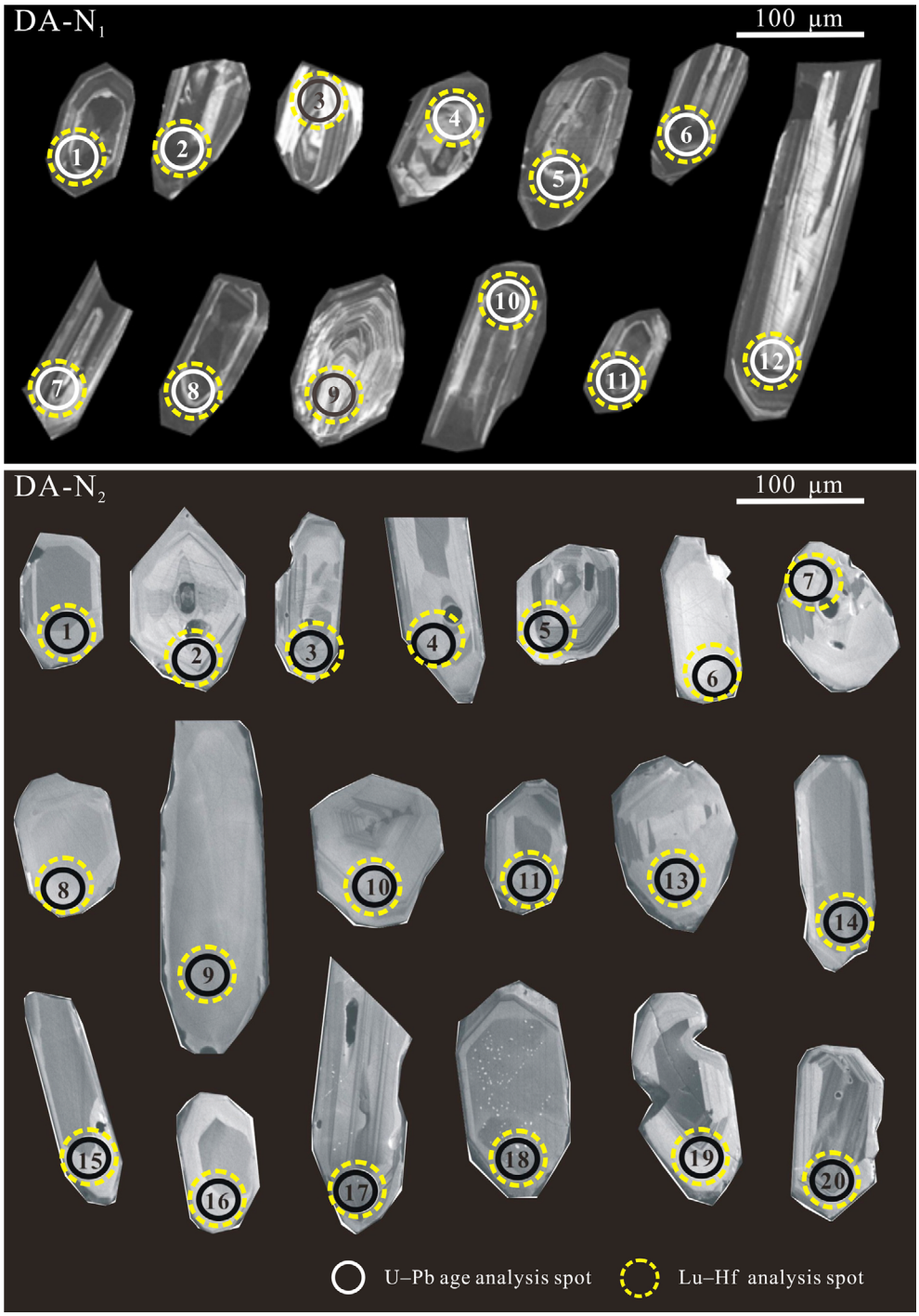

Fig. 6. Cathodoluminescence (CL) images of selected zircons for the trachyandesites from the Dong'an Au mining area.

N_2: 0.58–1.55), indicative of a magmatic origin (Li et al., 2009). Zircons from sample DA-N_1 yield a concordant zircon U-Pb age of 108.0 ± 1.1 Ma (MSWD = 0.91) (Fig. 7a). Zircons from DA-N_2 yield a concordant U-Pb age of 104.7 ± 4.3 Ma (MSWD = 17) (Fig. 7b), two older ages may represent the timing of formation of captured zircon grains that were entrained by the trachyandesite.

4.3. Zircon Hf Isotopes

Since the zircons generally have low $^{176}Lu/^{177}Hf$ ratios and the ^{176}Lu has a relatively long half-life, the insignificant amounts of radiogenic ^{176}Hf of the samples are negligible and the measured $^{176}Lu/^{177}Hf$ ratios basically represents its initial formation value. Nearly all of the zircon U-Pb dating spots from sample DA-N_1

https://doi.org/10.1007/s12303-021-0012-8

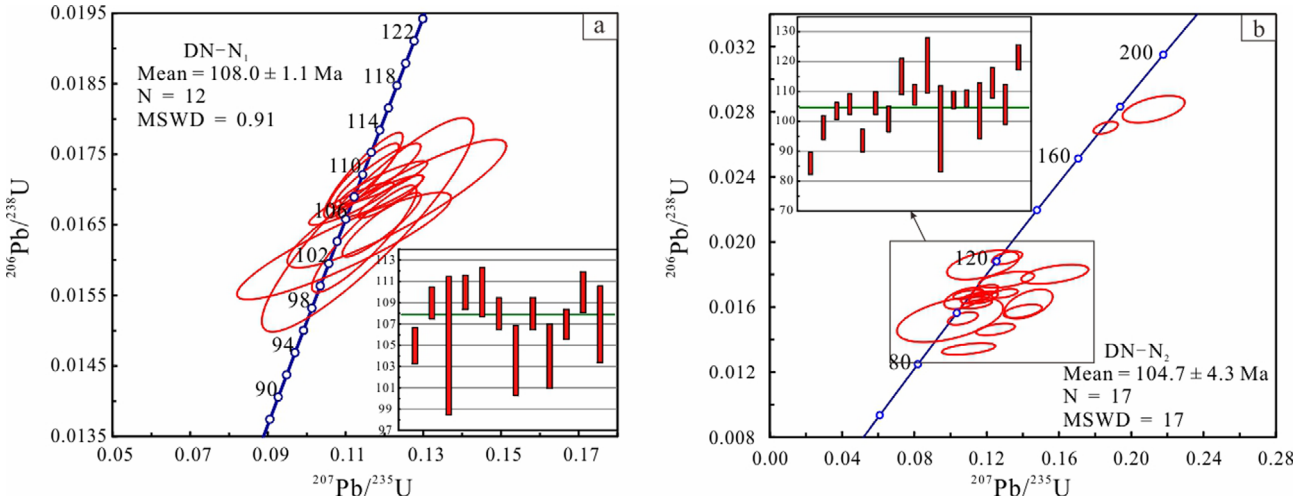

Fig. 7. Zircon U-Pb concordia and weighted diagrams for the trachyandesites from the Dong'an Au mining area.

and DA-N_2 are also chosen for in situ Hf isotope analysis, and the results of which are listed in Table S3 (electronic supplementary material). These zircons for sample DA-N_1 and sample DA-N_2 have $^{176}Hf/^{177}Hf$ ratios of 0.282623–0.282748 and 0.282630–0.282772, respectively; their $\varepsilon_{Hf}(t)$ values vary from –3.2 – 1.2 and –2.3 – 2.6, and corresponding to two-stage model ages (T_{DM2}) of 1372–1090 Ma and 1321–1009 Ma, respectively.

5. DISCUSSION

5.1. Magma Source and Petrogenesis

The samples have similar major and trace elements and isotopic compositions, indicating that all of them derived from the same magma source. They have Nb/Ta average ratios of 9.96, consistent with the Nb/Ta ratio of magmas derived from the melting of crustal material (11–12; Green, 1995). The low Cr, Ni, Co and lower $Mg^{\#}$ values of the samples also do not support the mantle source of magma. They have a wide range of Rb/Sr ratios cluster between 0.10 and 0.19, that is close to the average composition of the lower crust material (0.17) but is much higher than the average Rb/Sr ratio of the mantle (0.034; Sun and McDonough, 1989). The samples have the Th/La ratio of 0.164–0.289 (average of 0.233), Th/Nb ratio of 0.395–0.987 (average of 0.717), and La/Nb ratio of 2.35–3.37, similar to the ratio of crustal material (the average ratio of the continental crust and the original mantle, respectively: La/Nb is 2.2 and 0.94, Th/Nb is 0.44 and 0.177, Th/La is 0.204 and 0.125, Saunders et al., 1988; Weaver, 1991). In short, all data suggest that the trachyandesite associated with the Dong'an deposit were derived from a crustal source.

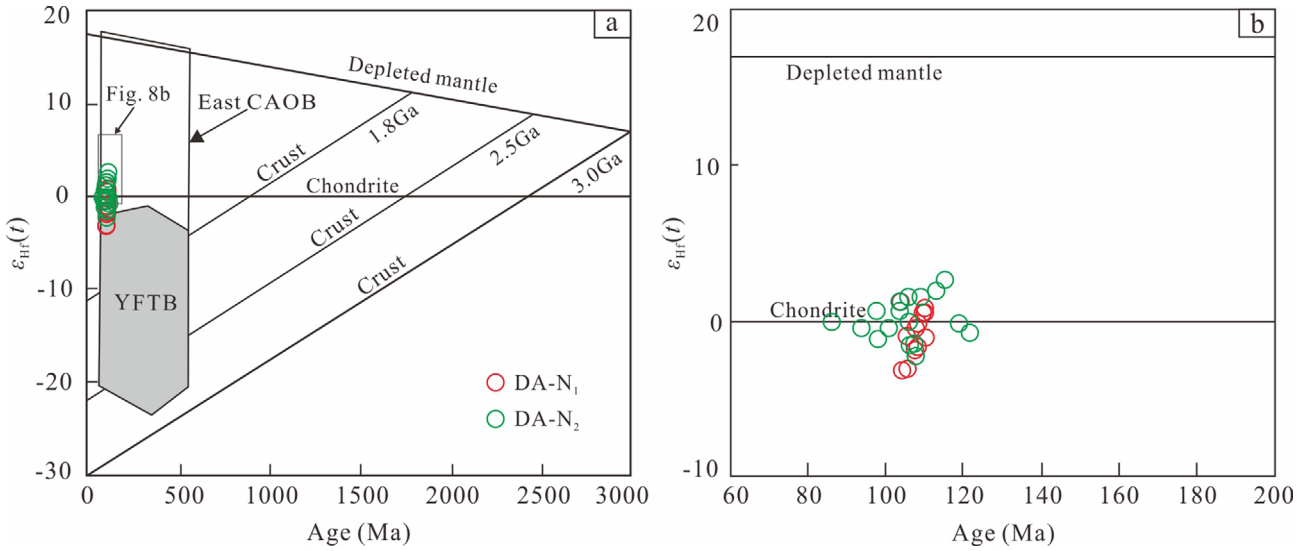

Fig. 8. Plots of zircon U-Pb ages-$\varepsilon_{Hf}(t)$ values for the trachyandesites from the Dong'an Au mining area.

Hf isotope features of zircons can provide great constraints on magma source (Griffin et al., 2002; Wu et al., 2007). The depleted mantle and juvenile crustal materials generally have higher $^{176}Hf/^{177}Hf$ ratios and positive $\varepsilon_{Hf}(t)$ values (Sui et al., 2007), whereas the ancient crustal materials and enriched mantle commonly have lower $^{176}Hf/^{177}Hf$ ratios and negative $\varepsilon_{Hf}(t)$ values (Veryoort et al., 1996). The zircon positive $\varepsilon_{Hf}(t)$ values of the granitic rocks are usually considered to be partially melted from the depleted mantle or from the juvenile crust that was derived from the depleted mantle. In contrast, the zircon negative $\varepsilon_{Hf}(t)$ values are generally indicative of partial melting of the crustal material (Wu et al., 2007).

The zircons $^{176}Hf/^{177}Hf$ ratios collected from the trachyandesite yield 0.282623–0.282748 and 0.282630–0.282772 (the samples DA-N_1 and DA-N_2, respectively), indicating a mixed origin of the depleted mantle or the juvenile crustal materials and the ancient crustal materials. The $\varepsilon_{Hf}(t)$ values vary from –3.2 – 1.2 and –2.3 – 2.6 (the samples DA-N_1 and DA-N_2, respectively) record a complex source environment that included not only the juvenile lower crust materials but also the ancient crustal materials, as evidenced by captured zircon grains with Early Jurassic ages. These samples plot in fields between the depleted mantle evolution line and the crustal evolution line on the T-$\varepsilon_{Hf}(t)$ diagram, also showing the mixed source of magma (Fig. 8).

The lithology of the Lower Cretaceous Fuminghe Formation volcanic rocks varies in a wide range, including andesite, trachyandesite,

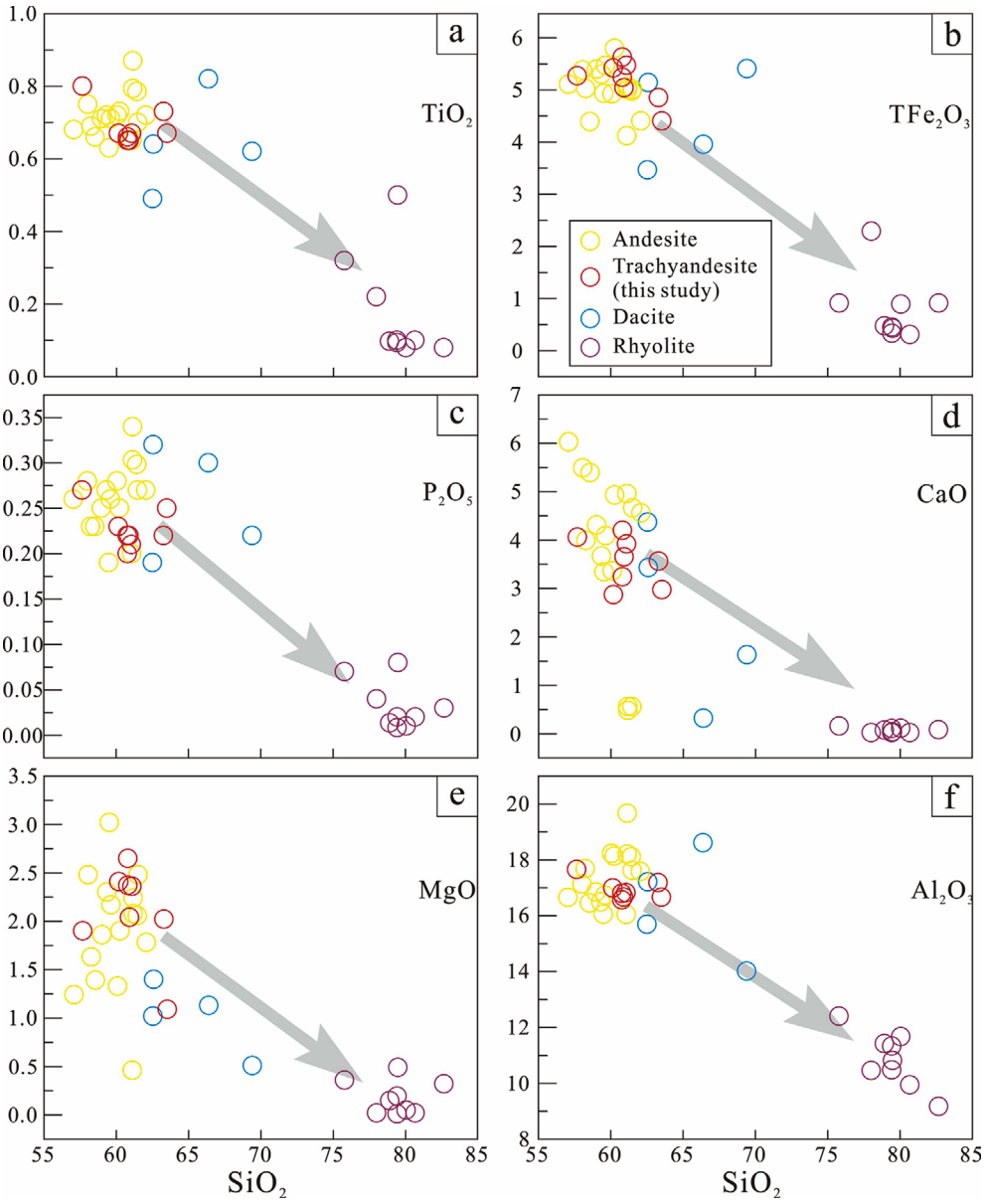

Fig. 9. Harker diagrams for the trachyandesites and the Lower Cretaceous Fuminghe Formation volcanic rocks from the Dong'an Au mining area. The data sources are the same as those in Figure 4.

https://doi.org/10.1007/s12303-021-0012-8

dacite and rhyolite (Fig. 2). Different volcanic rock lithologies coexist in space and have a continuous change trend of major and trace elements, suggesting that they may be the products of comagmatic evolution. The contents of Al_2O_3, MgO, TFe_2O_3, P_2O_5, CaO and TiO_2 decreased obviously with the increase of SiO_2 content, reflecting the existence of fractional crystallization in the process of magma evolution (Figs. 9a–f). The decrease of MgO and TFe_2O_3 content indicates the fractional crystallization of Mg-Fe-rich minerals (e.g., olivine, hornblende and orthopyroxene; Figs. 9b and e), while the decrease of CaO corresponds to the fractional crystallization of clinopyroxene and basic plagioclase (Fig. 9d). From intermediate to acidic volcanic rocks of the Lower Cretaceous Fuminghe Formation, the depletion degree of Nb, Ta, Ti, P, Sr and Eu gradually increased (Figs. 5a–d), indicating the fractional crystallization of Ti-Fe oxides, rutile, apatite and plagioclase. Therefore, we suggest that the andesite and trachyandesite of the Fuminghe Formation represent the initial intermediate magma formed by partial melting of the juvenile lower crust with involvement of the ancient crustal materials, and acidic volcanic rocks (e.g., dacite and rhyolite) were formed after fractional crystallization.

5.2. Implications for Tectonic Setting

The samples are enriched in LILEs, LREEs, and incompatible elements, depleted in HFSEs, indicating their formation in a volcanic arc setting (Liégeois et al., 1998). The samples plot in the volcanic arc field and near the continental crust field on a La/Nb-Ba/Nb discrimination diagram (Fig. 10a). And in the Sc/Ni-La/Yb diagram (Fig. 10b), all samples fall in Andeans-type field, which represents an environment of active continental margin. Besides, the volcanic rocks in this area are characterized by dominantly alkali-rich characteristics, indicating their formation in a subduction-related extensional tectonic setting (Li and Zhang, 2010). In addition, volcanic rocks that form within continental margins generally have higher alkali concentrations than those that form in island arc environments (Li, 2012), suggesting that the rocks in the study area formed in a continental arc environment.

The widespread late Mesozoic magmatic activities in NE China was controlled by both the closure of the Mongol-Okhotsk Ocean and the subduction of the Palaeo-Pacific Plate (Xu et al., 2013). The subduction of the Paleo-Pacific Plate beneath the NE China is generally considered to have started by the Early Jurassic (Wu et al., 2011; Yu et al., 2012; Ji et al., 2019), leading to the late Mesozoic volcanic activity in the Lesser Xing'an Range rather than the closure of the Mongol-Okhotsk Ocean (Xu et al., 2013). NE China was featured by a tectonic transition from compression to extension in Early Cretaceous (Zhang et al., 2010b; Lin et al., 2013; Ouyang et al., 2015; Sun et al., 2020). Early Cretaceous strong extension in NE China is indicated by contemporary metamorphic core complexes (Liu et al., 2005; Yang et al., 2007), A-type granites (Wu et al., 2002), bimodal volcanic rock combinations (Pei, 2005; Liu et al., 2020), and rift-basins (Wang et al., 2011) in NE China. Early Cretaceous tectonic transition induced an eastward younging magmatism (Zhang et al., 2010b; Shu et al., 2016), which is interpreted to be the result of the rollback of the subducted Paleo-Pacific Plate (Wu et al., 2011; Sun et al., 2013b; Shu et al., 2015; Tang et al., 2018). This led to asthenosphere upwelling and underplating (Fig. 11), resulting in Early Cretaceous strong magmatism, which were accompanied by numerous epithermal Au deposits (Fig. 1). The epithermal Au mineralization is generally controlled by volcanic edifices and deep-seated faults, and occurs during the waning stage of volcanic evolution (Fig. 11). The pyrite Rb-Sr isochron age of the Sandaowanzi Au deposit is

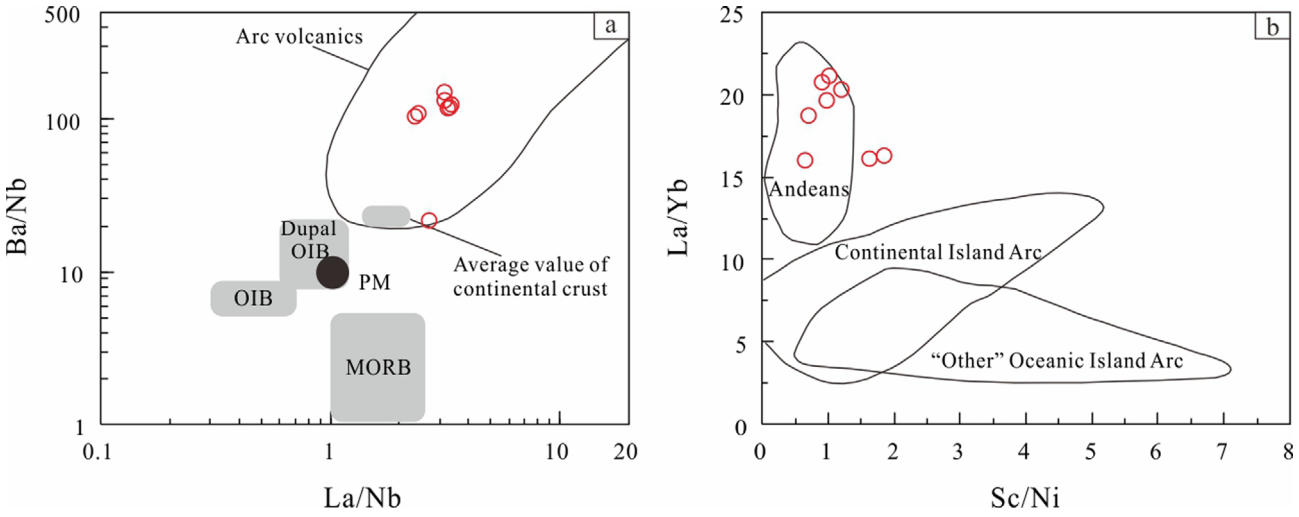

Fig. 10. La/Nb-Ba/Nb (a) and Sc/Ni-La/Yb (b) diagrams of tectonic environment for the trachyandesites from the Dong'an Au mining area.

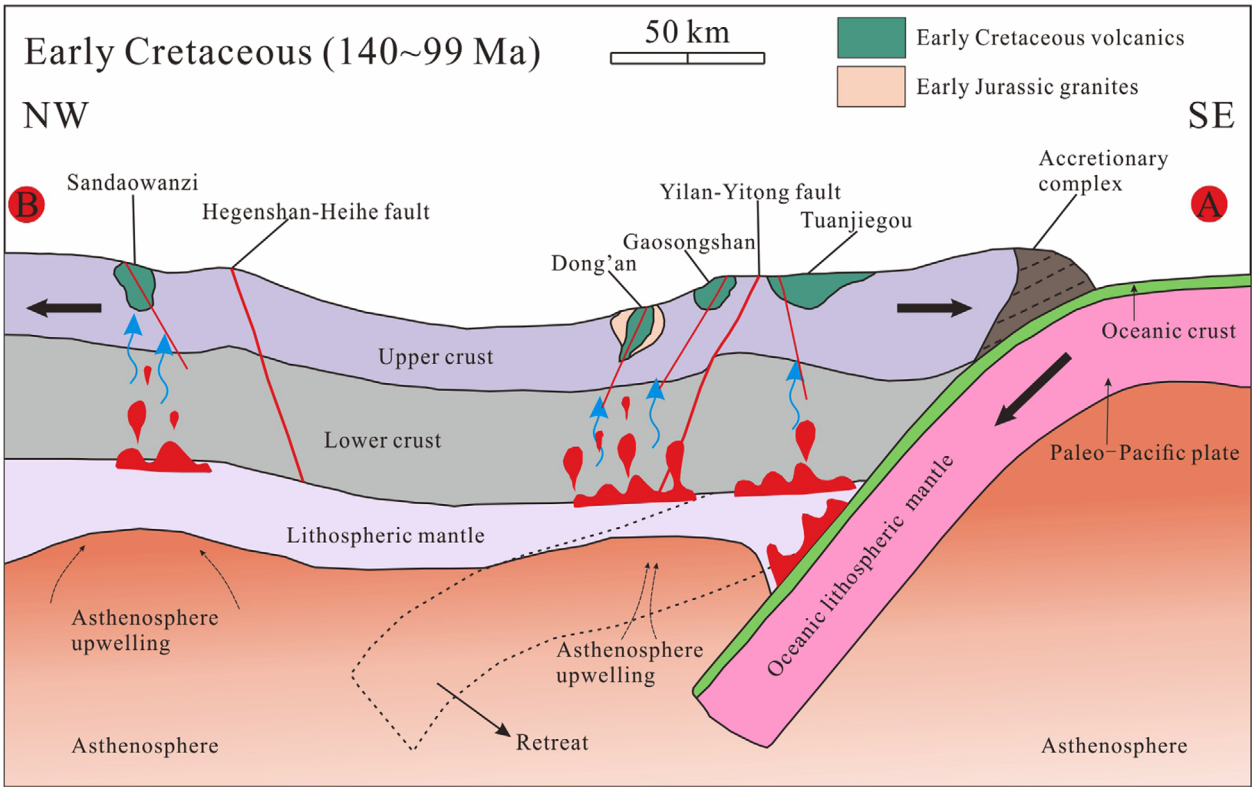

Fig. 11. Schematic model showing the genetic model and tectonic setting for the late Early Cretaceous epithermal Au mineralization in NE China.

119 ± 3.9 Ma (Zhai et al., 2015); the Dong'an Au deposit has a mineralization age (hydrothermal adularia $^{40}Ar/^{39}Ar$ plateau age) of 105.1 ± 0.7 Ma (a little younger than the age of the surrounding volcanic rocks; Xue, 2012); the U-Pb age of hydrothermal zircons from the Gaosongshan Au deposit is ca. 99 Ma (Hao et al., 2016). The decrease in mineralization age from west to east also can be interpreted as the result of the gradual eastward retreat of the subducted Paleo-Pacific Plate (Fig. 11). Our new geochronological data in this study are consistent with this viewpoint. Asthenosphere upwelling led to partial melting of mafic lower crust, generating the parental andesitic magmas, which had experienced a different degree of fractional crystallization to form the wide range of the Fuminghe Formation volcanic rocks (e.g., trachyandesites, dacites, and rhyolites).

6. CONCLUSIONS

Combined with previous geological and petrogeochemical studies on the volcanic rocks in the Dong'an Au deposit, petrogeochemical data presented in this study for the trachyandesites in the Dong'an Au deposit can reach the following conclusions:

(1) The zircon U-Pb ages of the trachyandesites (major surrounding rock) in the Dong'an Au deposit are 108–105 Ma, consistent with the adularia Ar-Ar age (105.1 ± 0.7 Ma).

(2) The volcanic rocks in the Dong'an Au deposit are comagmatic, fractional crystallization played an important role in the differentiation of the volcanic rocks from the andesite and trachyandesite to dacite and rhyolite.

(3) The trachyandesites in the Dong'an Au deposit were derived from partial melting of the juvenile lower crust with involvement of the ancient crustal materials, were likely formed during the retreat of the subducted Paleo-Pacific Plate.

ACKNOWLEDGMENTS

This paper was funded by the Nature Science Foundation of Jilin Province (No. 20180101089JC), the Key Project of Science and Technology Development Plan of Jilin Province (Grant No. 20100445), and the National Nature Science Foundation of China (Grant No. 41272093). Thanks the Key Laboratory of Mineral Resources Evaluation in Northeast Asia, Ministry of Land and Resources, Changchun, China for helping in major and trace element analyses.

REFERENCES

Anderson, T., 2002, Correction of common lead in U-Pb analyses that do not report ^{204}Pb. Chemical geology, 192, 59–79.

Bai, L.A., Sun, J.G., Zhang, Y., Han, S.J., Yang, F.C., Men, L.J., Gu, A.L.,

https://doi.org/10.1007/s12303-021-0012-8

and Zhao, K.Q., 2012, Genetic type, mineralization epoch and geodynamical setting of endogenous copper deposits in the Great Xing'an Range. Acta Petrologica Sinica, 28, 468–482. (in Chinese with English abstract)

Boynton, W.V., 1984, Cosmochemistry of the rare earth elements: meteorites studies. In: Henderson, P. (ed.), Rare Earth Element Geochemistry. Elsevier, Amsterdam, 2, p. 63–114. https://doi.org/10.1016/B978-0-444-42148-7.50008-3

Chen, J., 2011, Metallogenic setting and metallogenesis of nonferrous-precious metals in Lesser Hinggan Mountain, Heilongjiang Province. Ph.D. Thesis, Jilin University, Changchun, 158 p. (in Chinese with English abstract)

Chen, Y.J., Zhang, C., Li, N., Yang, Y.F., and Deng, K., 2012, Geology of the Mo deposits in northeast China. Journal of Jilin University (Earth Science Edition), 42, 1223–1268. (in Chinese with English abstract)

Green, T.H., 1995, Significance of Nb/Ta as an indicator of geochemical processes in the crust-mantle system. Chemical Geology, 120, 347–359.

Griffin, W.L., Wang, X., Jackson, S.E., Pearson, N.J., O'Reilly, S.Y., Xu, X.S., and Zhou, X.M., 2002, Zircon chemistry and magma mixing, SE China: in-situ analysis of Hf isotopes, Tonglu and Pingtan igneous complexes. Lithos, 61, 237–269.

Guo, J.H., Wang, C.S., and Shi, Y.J., 2004, Geological and geochemical features of the Dong'an gold deposit in Heilongjiang. Geology and Prospecting, 40, 36–41. (in Chinese with English abstract)

Hao, B.W., Deng, J., Bagas, L., Ge, L.S., Nie, F.J., Turner, S., and Qing, M., 2016, The Gaosongshan epithermal gold deposit in the lesser Hinggan range of the Heilongjiang Province, NE China: implications for early Cretaceous mineralization. Ore Geology Reviews, 73, 179–197.

Hu, Z.C., Gao, S., Liu, Y.S., Hu, S.H., Chen, H.H., and Yuan, H.L., 2008a, Signal enhancement in laser ablation ICP-MS by addition of nitrogen in the central channel gas. Journal of Analytical Atomic Spectrometry, 23, 1093–1101.

Hu, Z.C., Liu, Y.S., Gao, S., Hu, S.H., Dietikerc, R., and Günther, D., 2008b, A local aerosol extraction strategy for the determination of the aerosol composition in laser ablation inductively coupled plasma mass spectrometry. Journal of Analytical Atomic Spectrometry, 23, 1192–1203.

Huo, L. and Sun, F.Y., 2010, Study on the characteristics of fluid inclusions and implications for deposit genesis of Dong'an gold deposit, Heilongjiang province. Gold, 31, 8–14. (in Chinese with English abstract) https://doi.org/10.3969/j.issn.1001-1277.2010.03.003

Irvine, T.H. and Baragar, W.R.A., 1971, A guide to the chemical classification of the common volcanic rocks. Canadian Journal of Earth Sciences, 8, 523–548.

Ji, Z., Meng, Q.A., Wan, C.B., Zhu, D.F., Ge, W.C., Zhang, Y.L, Yang, H., and Dong, Y., 2019, Geodynamic evolution of flat-slab subduction of Paleo-Pacific Plate: constraints from Jurassic adakitic lavas in the Hailar Basin, NE China. Tectonics, 38, 4301–4319. https://doi.org/10.1029/2019TC005687

Li, B.M, 2012, Geochemistry and tectonic background of the volcanic rocks of Early Carboniferous Maergenhe Formation in Nenjiang area, Heilongjiang Province. M.S. Thesis, Jilin University, Changchun, 51 p. (in Chinese with English abstract)

Li, B.L. and Zhang, H., 2010, Some advances in the research of epithermal gold deposits. Mineralogica Sinica, 30, 90–97. (in Chinese with English abstract)

Li, H.K., Gen, J.Z., Hao, S., Zhang, Y.Q., and Li, H.M, 2009, Research on the dating zircon U-Pb age by LA-MC-ICPMS. Bulletin of Mineralogy, Petrology and Geochemistry, 28, 77. (in Chinese with English abstract)

Li, Y.L., Zhou, H.W., Xiao, W.J., Zhong, Z.Q., Yin, S.P., and Li, F.L., 2012, Superposition of Paleo-Asian and West-Pacific tectonic domains in the eastern section of the Solonker suture zone: insights from petrology, geochemistry and geochronology of deformed diorite in Xar Moron fault zone, Inner Mongolia. Earth Science, 37, 433–450. (in Chinese with English abstract)

Liégeois, J.P., Navez, J., Hertogen, J., and Black, R., 1998, Contrasting origin of post-collisional high-K calc-alkaline and shoshonitic versus alkaline and peralkaline granitoids, the use of sliding normalization. Lithos, 45, 1–28.

Lin, W., Faure, M., Chen, Y., Ji, W.B., Wang, F., Wu, L., Charles, N., Wang, J., and Wang, Q.C., 2013, Late Mesozoic compressional to extensional tectonics in the Yiwulüshan massif, northeastern China and its bearing on the evolution of the Yinshan-Yanshan orogenic belt: Part I: Structural analyses and geochronological constraints. Gondwana Research, 23, 54–77.

Liu, J.L., Davis, G.A., Lin, Z.Y., and Wu, F.Y., 2005, The Liaonan metamorphic core complex, southeastern Liaoning Province, North China: a likely contributor to Cretaceous rotation of eastern Liaoning, Korea and contiguous areas. Tectonophysics, 407, 65–80.

Liu, R.P., Gu, X.X., Zhang, Y.M., Wang, J.L., Zheng, G., and Gao, H.J., 2015, Zircon U-Pb geochronology and petrogeochemistry of host igneous rocks of the Dong'an gold deposit in Heilongjiang Province, NE China. Acta Petrologica Sinica, 31, 1391–1408.

Liu, Y., Chu, X.L., Sun, J.G., Han, J.L., Ren, L., Gu, A., Zhao, K.Q., and Zhao, C.T., 2020, Early Cretaceous bimodal magmatism related epithermal mineralization: a case study of the Gaosongshan gold deposit in the northern Lesser Xing'an Range, NE China. Ore Geology Reviews, 121, 103563.

Liu, Y., Sun, J.G., Han, J.L., Ren, L., Gu, A., Zhao, K.Q., Feng, Y.Y., and Chu, X.L., 2021, Constraints of magmatic differentiation on epithermal mineralization at Dongan, NE China: insights from zircon geochronology, elements and Sr-Hf-Nd isotope geochemistry. Journal of Geochemical Exploration, 55, 106768.

Liu, Y.S., Gao, S., Hu, Z.C., Gao, C.G., Zong, K.Q., and Wang, D.B., 2010, Continental and oceanic crust recycling-induced melt-peridotite interactions in the Trans-North China Orogen: U-Pb dating, Hf isotopes and trace elements in zircons from mantle xenoliths. Journal of Petrology, 51, 537.

Liu, Y.S., Hu, Z.C., Gao, S., Günther, D., Xu, K.J., Gao, C.G., and Chen, H.H., 2008, In situ analysis of major and trace elements of anhydrous minerals by LA-ICP-MS without applying an internal standard. Chemical Geology, 257, 34–43.

Ludwig, K.R., 2003, User's manual for Isoplot/EX version 3.0: a geochronological toolkit for Microsoft Excel. Berkeley Geochronology Center, Special Publications, 4, 70 p.

Ouyang, H.G., Mao, J.W., Zhou, Z.H., and Su, H.M., 2015, Late Meso-

zoic metallogeny and intracontinental magmatism, southern Great Xing'an Range, northeastern China. Gondwana Research, 27, 1153–1172.

Peccerillo, A. and Taylor, S.R., 1976, Geochemistry of Eocene calc-alkaline volcanic rocks from the Kastamonu area, northern Turkey. Contributions to Mineralogy and Petrology, 58, 63–81.

Pei, F.P., 2005, Petrology and geochemistry of Mesozoic volcanic rocks in southern Jilin Province. M.S. Thesis, Jilin University, Changchun, 68 p. (in Chinese with English abstract)

Rudnick, R.L., Gao, S., Ling, W.L., Liu, Y.S., and McDonough, W.F., 2004, Petrology and geochemistry of spinel peridotite xenoliths from Hannuoba and Qixia, North China craton. Lithos, 77, 609–637.

Saunders, A.D., Norry, M.J., and Tarney, J., 1988, Origin of MORB and chemically-depleted mantle reservoirs: trace element constraints. Journal of Petrology, Special Volume, 415–445. https://doi.org/10.1093/petrology/Special_Volume.1.415

Shu, Q.H., Chang, Z.S., Lai, Y., Zhou, Y.T., Sun, Y., and Yan, C., 2016, Regional metallogeny of Mo-bearing deposits in northeastern China, with new Re-Os dates of porphyry Mo deposits in the northern Xilamulun district. Economic Geology, 111, 1783–1798.

Shu, Q.H., Lai, Y., Zhou, Y.T., Xu, J.J., and Wu, H.Y., 2015, Zircon U-Pb geochronology and Sr-Nd-Pb-Hf isotopic constraints on the timing and origin of Mesozoic granitoids hosting the Mo deposits in northern Xilamulun district, NE China. Lithos, 238, 64–75.

Su, R.K., Yu, J.B., Zhu, Y.J., and Song, C.B., 2006, Geological characteristics and prospecting potential of Dongan gold ore field in Heilongjiang. Gold Science and Technology, 14, 10–13. (in Chinese with English abstract)

Sui, Z.M., Ge, W.C., Wu, F.Y., Zhang, J.H., Xu, X.C., and Cheng, R.Y., 2007, Zircon U-Pb ages, geochemistry and its petrogenesis of Jurassic granites in northeastern part of the Da Hinggan Mts. Acta Petrologica Sinica, 23, 461–480. (in Chinese with English abstract)

Sun, J.G., Zhang, Y., Han, S.J., Men, L.J., Li, Y.X., Chai, P., and Yang, F., 2013a, Timing of formation and geological setting of low-sulphidation epithermal gold deposits in the continental margin of NE China. International Geology Review, 55, 608–632.

Sun, M.D., Chen, H.L., Zhang, F.Q., Wilde, S.A., Dong, C.W., and Yang, S.F., 2013b, A 100 Ma bimodal composite dyke complex in the Jiamusi Block, NE China: an indication for lithospheric extension driven by Paleo-Pacific roll-back. Lithos, 162–163, 317–330.

Sun, S.S. and McDonough, W.F., 1989, Chemical and isotopic systematics of oceanic basalts: implications for mantle composition and processes. In: Saunders, A.D. and Norry, M.J. (eds.), Magmatism in the Ocean Basins. Geological Society, London, Special Publications, 42, p. 313–345.

Sun, Y.G., Li, B.L., Sun, F.Y., Ding, Q.F., Wang, B.Y., Li, Y.J., and Wang, K., 2020, Mineralization events in the Xiaokele porphyry Cu (-Mo) deposit, NE China: evidence from zircon U-Pb and K-feldspar Ar-Ar geochronology and petrochemistry. Resource Geology, 70, 254–272.

Tang, J., Xu, W.L., Wang, F., and Ge, W.C., 2018, Subduction history of the Paleo-Pacific slab beneath Eurasian continent: Mesozoic–Paleogene magmatic records in Northeast Asia. Science China Earth Sciences, 61, 527–559.

Vervoort, J.D. and Patchett, P.J., 1996, Behavior of hafnium and neodymium isotopes in the crust: constraints from Precambrian crustally derived granites. Geochimica et Cosmochimica Acta, 60, 3717–3733.

Wang, T., Zheng, Y.D., Zhang, J.J., Zeng, L.S., Donskaya, T., and Guo, L., Li, J.B., 2011, Pattern and kinematic polarity of late Mesozoic extension in continental NE Asia: perspectives from metamorphic core complexes. Tectonics, 30, TC6007. https://doi.org/10.1029/2011TC002896

Weaver, B.L., 1991, The origin of ocean island basalt end member compositions: trace element and isotopic constraints. Earth and Planetary Science Letters, 101, 381–397.

Wen, S., Li, B.L., Li, L.B., and Wang, B., 2013, Zircon U-Pb age and geochemistry of Nanquanyan diorite in the Lanjia gold deposit, Jilin Province. Earth Science-Journal of China University of Geosciences, 38, 305–315. (in Chinese with English abstract)

Wu, F.Y., Li, X.H., Zheng, Y.F., and Gao, S., 2007, Lu-Hf isotopic systematics and their applications in petrology. Acta Petrologica Sinica, 23, 185–220. (in Chinese with English abstract)

Wu, F.Y., Sun, D.Y., Ge, W.C., Zhang, Y.B., Grant, M.L., Wilde, S.A., and Jahn, B.M., 2011, Geochronology of the Phanerozoic granitoids in northeastern China. Journal of Asian Earth Sciences, 41, 1–30.

Wu, F.Y., Sun, D.Y., Li, B.M., Jahn, B.M., and Wilde, S., 2002, A-type granites in northeastern China: age and geochemical constraints on their petrogenesis. Chemical Geology, 187, 143–173

Xu, W.L., Pei, F.P., Wang, F., Meng, E., Ji, W.Q., Yang, D.B., and Wang, W., 2013, Spatial-temporal relationships of Mesozoic volcanic rocks in NE China: constraints on tectonic overprinting and transformations between multiple tectonic regimes. Journal of Asian Earth Sciences, 74, 167–193.

Xue, M.X., 2012, Metallogenesis of endogenic gold deposits in Heilongjiang Province. Ph.D. Thesis, Jilin University, Changchun, 164 p. (in Chinese with English abstract)

Xue, M.X., Sun, F.Y., Li, B.L., and Ding, Q.F., 2012, Discovery, exploration and inspiration of No. 5 gold lode in Dong'an large-scale gold deposit, Heilongjiang. Gold, 5, 6–11. (in Chinese with English abstract)

Xue, M.X., Ye, S.Q., Liu, Z.M., Yang, Z.W., Guo, J.H., Su, R.K., and Chen, H.M., 2002, The geology and geochemistry of the Dong'an gold deposit in Heilongjiang Province. Gold, 23, 1–3. (in Chinese with English abstract)

Yang, J.H., Wu, F.Y., Chung, S.L., Lo, C.H., Wilde, S.A., and Davis, G.A., 2007, Rapid exhumation and cooling of the Liaonan metamorphic core complex: inferences from $^{40}Ar/^{39}Ar$ thermochronology and implications for Late Mesozoic extension in the eastern North China Craton. Geological Society of America Bulletin, 119, 1405–1414.

Ye, X., 2011, Study on geological characteristics and genesis of Dongan gold deposit, Xunke county, Heilongjiang Province. M.S. Thesis, Jilin University, Changchun, 64 p. (in Chinese with English abstract)

Yu, J.J., Wang, F., Xu, W.L., Gao, F.H., and Pei, F.P., 2012, Early Jurassic mafic magmatism in the Lesser Xing'an–Zhangguangcai Range, NE China, and its tectonic implications: constraints from zircon U-Pb chronology and geochemistry. Lithos, 142–143, 256–266.

Yuan, H.L., Gao, S., and Liu, X.M., 2004, Accurate U-Pb age and trace element determinations of zircon by laser ablation inductively coupled plasma mass spectrometry. Geostandards and Geoanalytical Research, 28, 353–370.

Zhai, D.G., Liu, J.L., Ripley, E.M., Wang, J.P., and Tian, S.H., 2015, Geochronological and He-Ar-S isotopic constraints on the origin of the

Sandaowanzi gold-telluride deposit, northeastern China. Lithos, 212–215, 338–352.

Zhang, J.H., Gao, S., Ge, W.C., Wu, F.Y., Yang, J.H., Wilde, S.A., and Li, M., 2010b, Geochronology of the Mesozoic volcanic rocks in the Great Xing'an Range, northeastern China: implications for subduction-induced delamination. Chemical Geology, 276, 144–165.

Zhang, Z.C., Mao, J.W., Wang, Y.B., Pirajno, F., Liu, J.L., and Zhao, Z.D, 2010a, Geochemistry and geochronology of the volcanic rocks associated with the Dong'an adularia-sericite epithermal gold deposit, Lesser Hinggan Range, Heilongjiang province, NE China: constraints on the metallogenesis. Ore Geology Reviews, 37, 158–174.

Zhi, Y.B., Li, B.L., Xi, A.H., Xu, Q.L., Zhang, L., Sun, Y.G., Chang, J.J., and Peng, B., 2016, Geochronology and geochemistry of the major host rock of the Dong'an gold deposit, Lesser Khingan Range: implications for petrogenesis and metallogenic setting during the Early–Middle Jurassic in northeast China. Geochemistry, 76, 257–274.

Publisher's Note Springer Nature remains neutral with regard to jurisdictional claims in published maps and institutional affiliations.